Journal of Solid Mechanics Vol. 8, No. 1 (2016) pp. 212-231

Free Vibration Analysis of Continuously Graded Fiber Reinforced Truncated Conical Shell Via Third-Order Shear Deformation Theory

M.H. Yas [1,*], M. Nejati [1] ,A. Asanjarani [2]

[1]*Mechanical Engineering Department, Razi University, Kermanshah, Iran*
[2]*Department of Mechanical Engineering, Islamic Azad University, Arak Branch, Iran*

Received 15 January 2016; accepted 20 March 2016

ABSTRACT

This paper deals with free vibration analysis of continuously graded fiber reinforced (CGFR) truncated conical shell based on third-order shear deformation theory (TSDT), by developing special power-law distributions. The orthotropic (CGFR) truncated conical shell are clamped and simply supported at the both ends. It is assumed to have a smooth variation of fibers volume fraction in the thickness direction. Symmetric and classic volume fraction profiles are examined. The appropriate displacement functions which identically satisfy the axisymmertic conditions are used to simplify the motion equations to a set of coupled ordinary differential equation with variable coefficients, which can be solved by generalized differential quadrature method (GDQM), to obtain the natural frequencies. The fast rate of convergence of the method is observed. To validate the results, comparisons are made with the available solutions for isotropic and CGM isotropic truncated conical shells. The effect of various geometrical parameters on the vibrational behavior of the CGFR truncated conical shell is investigated. This literature mainly contributes to illustrate the impact of the power-law distributions on the vibrarional behavior of orthotropic continuous grading truncated conical shell. This paper is also supposed to present useful results for continuouly graded fibers volume fraction in the thickness direction of a truncated conical shell and comparison with similar discrete laminated composite one.

Keywords : Continuously graded fiber reinforced; Special power-law distributions; Truncated conical shell; Free vibration; TSDT.

1 INTRODUCTION

TRUNCATED conical shells are extensively employed in a wide range of engineering fields due to their special geometric shapes. Thus, the investigation of their vibrational behavior has been interesting for designers. Moreover, because of the needs to apply in severe high temperature environments, usage of continuous grading truncated conical shell has become more and more common. One of the advantages of CGMs is that one can design directional properties into them almost on demand. CGMs are heterogeneous materials and have properties that vary constantly as a function of position within the material. CGM is created by smoothly changing the volume fraction of its constituent materials. Compared with the analysis of continuous grading plates (Malekzadeh [1], Hosseini-Hashemi et al.[2], Pan and Han [3], Yas and SobhaniAragh [4]) and continuous grading spheres (Chen [5],

*Corresponding author. Tel.: +98 831 4274538; Fax: +98 831 4274542.
E-mail address: yas@razi.ac.ir (M.H. Yas).

Chiroiu and Munteanu [6]) as well as continuous grading cylindrical shells (Bahtui and Eslami 2007[7], Haddadpour et al. 2007[8], SobhaniAragh and Yas [9-11], Yas and SobhaniAragh [12]), the investigation of continuous grading truncated conical shell is limited in number.

Thambiratnam, and Zhuge [13] presented a simple finite element method for the axial symmetry of free vibration analysis of conical shells with uniform or varying wall thickness. Tong [14] used a particularly convenient coordinate system, a simple and obtained exact solution for the Donnell-type governing equations of the free vibration of composite laminated conical shells, with orthotropic stretching-bending coupling. The solution was in the form of a power series. Leissa [15] investigated the effects of semi-vertex angles and different boundary conditions on the frequency behavior of conical shells. Liew and Lim [16] studied the vibration analysis of shallow conical shells via a global Ritz formulation based on the energy principle. Next (Liew and Lim [17]), a formulation for the free vibration of moderately thick conical shell panels founded on shear deformable theory was also offered by them. The Generalized Differential Quadrature Method was employed to investigate the free vibration of composite laminated conical shells by Shu [18].The vibration characteristics of open conically curved, isotropic shell panels using a h–p version of finite element method was studied by Bardell et al. [19]. Wang et al. [20] presented the procedures in which the DQM is applied to the study of free vibration of truncated conical shells with a variety of boundary conditions based on Love's first approximation theory. The stability of truncated conical shells of continuous grading material subjected to external pressure was investigated by Sofiyev [21]. Liew et al. [22] considered the free vibration analysis of thin conical shells under different boundary conditions based on the classical thin-shell theory. The analysis was carried out using the element-free kp-Ritz method.

Bhangale et al. [23] presented a finite element formulation based on First-Order Shear Deformation Theory (FSDT) to study the thermal buckling and vibrational behavior of truncated FGM conical shells in a high-temperature environment.

Tornabene [24] studied the dynamic behavior of moderately thick functionally graded conical with a four-parameter power-law distribution based on the First-order Shear Deformation Theory (FSDT). Materials were assumed to be isotropic and inhomogeneous through the thickness direction. Malekzadeh et al. [25] Investigated a three-dimensional (3D) free vibration analysis of the functionally graded (FG) truncated conical shells subjected to thermal environment. The material properties are assumed to be temperature dependent and graded in the radius direction. The differential quadrature method (DQM) as an efficient and accurate numerical tool is adopted to solve the thermal and thermo-mechanical governing equations. Sofiyev [26] studied the non-linear vibration of truncated conical shells made of functionally graded materials using the large deformation theory with von Karman–Donnell-type of kinematic non-linearity. The material properties of FGMs are assumed to vary continuously through the thickness of the shell. SobhaniAragh and Yas [9] studied static and free vibration characteristics of continuous grading fiber-reinforced (CGFR) cylindrical shells are considered based on the three-dimensional theory of elasticity, by making use of a generalized power-law distribution. They presented formulation, the cylindrical shell was assumed to be made of an orthotropic material. These authors (SobhaniAragh and Yas [10]) studied; three-dimensional analysis of thermal stresses in four-parameter continuously graded fiber reinforced cylindrical panel subjected to thermal load is studied. The cylindrical panel was assumed to be made of an orthotropic material. The continuously graded fiber reinforced panel had a smooth variation in matrix volume fraction in the radial direction. In the above mentioned papers, the material mostly assumed isotropic CGM conical shells, but in some practical usage, some materials are orthotropic. This research is motivated by lack of researches concerning to the effect of the parameters of power-law distributions on the vibration behavior of orthotropic continuous grading truncated conical shell. The purpose of this present study is to obtain free vibration solution for CGFR truncated conical shell with power-law distribution.CGFRs are new composite materials that are microscopically inhomogeneous and the mechanical properties vary continuously in one direction. This is achieved by gradually changing the volume fraction of the fiber reinforcement in the thickness direction, to obtain smooth variation of material properties and optimum response which is great advantage over discrete laminated structures. To the authors' best knowledge, there is not investigation in the open literature for free vibration of CGFR truncated conical shell which is made of orthotropic material, and no results for continuous grading of matrix volume fraction in the thickness direction of a truncated conical shell are available. In this study, influence of continuous grading of fiber reinforcement (CGFR) and choice of the power-law distributions of fibers on the vibration behavior of CGFR truncated conical shell is illustrated. Moreover, numerical results of CGFR truncated conical shells with arbitrary variation of volume fraction reinforcement in the shell's thickness compared with discretely laminated composite truncated conical shell. Although, in this paper the considered theory in comparison with the previous literatures, which were mostly based on the first- order shear deformation theory, is optimized and for achieving more precise results, third order shearing deformation theory is employed to achieve governing equations in this study.

2 PROBLEM FORMULATIONS

In this section, geometry, volume fraction distribution in thickness direction for orthotropic FGM, and governing equations of motion for truncated conical shell are described.

2.1 CGFR material properties

Consider a CGFR truncated conical shell with constant thickness *h* as shown in Fig. 1. Let (r,θ,z) coordinate system be located on the middle surface of the shell in the unstressed reference configuration. The coordinate *x* is measured along the cone generator with origin at the semi-vertex, the angle θ is the circumferential coordinate, and *z* is the thickness coordinate. Let R_1 and R_2 denote the radii of the truncated cone at small and large edges, respectively. α is the semi-vertex angle of the truncated cone and *L* is truncated cone length along *x* direction. If *R* denotes the radius of the truncated cone at any point along the *x* direction, then:

$$R = x\sin(\alpha) \qquad L_1 < x < L_2 \tag{1}$$

Linear strain–displacement relation is assumed. Furthermore, by using third-order shear deformation shell theory, displacement fields can be written as (Reddy [27]):

$$\begin{aligned} U(x,\theta,z,t) &= U_0(x,\theta,t) + z\,\Psi_x(x,\theta,t) + z^2\Phi_x(x,\theta,t) + z^3\eta_x(x,\theta,t) \\ V(x,\theta,z,t) &= V_0(x,\theta,t) + z\,\Psi_\theta(x,\theta,t) + z^2\Phi_\theta(x,\theta,t) + z^3\eta_\theta(x,\theta,t) \\ W(x,\theta,z,t) &= W_0(x,\theta,t) \end{aligned} \tag{2}$$

where U_0, V_0 denote the in-plane displacements on the mid-plane, W_0 is the transverse displacement, Ψ_x, Ψ_θ are the slopes of the normal to the mid-surface in the $\theta - z$ and $x - z$ surfaces, respectively, $\Phi_i, \eta_i\ (i = x,\theta)$ are the higher-order displacement parameters defined at the mid-plane, and *t* is the time.

Strain–displacement relations for truncated conical shell are expressed as:

$$\begin{aligned} &\varepsilon_x = \frac{\partial U}{\partial x}, \quad \varepsilon_\theta = \frac{1}{x\sin\alpha}\left\{U\sin\alpha + \frac{\partial V}{\partial\theta} + W\cos\alpha\right\}, \quad \gamma_{zx} = \frac{\partial U}{\partial z} + \frac{\partial W}{\partial x} \\ &\gamma_{x\theta} = \frac{1}{x\sin\alpha}\left\{\frac{\partial U}{\partial\theta} - V\sin\alpha\right\} + \frac{\partial V}{\partial x}, \quad \gamma_{z\theta} = \frac{\partial V}{\partial z} + \frac{1}{x\sin\alpha}\left\{\frac{\partial W}{\partial\theta} - V\cos\alpha\right\} \end{aligned} \tag{3}$$

By setting $\alpha = 0$, semi-vertex angle of the truncated conical shell formulation can be reduced to the formulation of cylindrical shells. Besides, the present formulation is also applicable to the analysis of annular plates by letting $\alpha = \pi/2$.

The mechanical constitutive relation that relates the stresses to the strains in this coordinate can be explained as:

$$\begin{Bmatrix} \sigma_x \\ \sigma_\theta \\ \sigma_z \\ \sigma_{z\theta} \\ \sigma_{zx} \\ \sigma_{x\theta} \end{Bmatrix} = \begin{bmatrix} C_{11} & C_{12} & C_{13} & 0 & 0 & 0 \\ C_{12} & C_{22} & C_{23} & 0 & 0 & 0 \\ C_{13} & C_{23} & C_{33} & 0 & 0 & 0 \\ 0 & 0 & 0 & C_{44} & 0 & 0 \\ 0 & 0 & 0 & 0 & C_{55} & 0 \\ 0 & 0 & 0 & 0 & 0 & C_{66} \end{bmatrix} \begin{Bmatrix} \varepsilon_x \\ \varepsilon_\theta \\ \varepsilon_z \\ \gamma_{z\theta} \\ \gamma_{zx} \\ \gamma_{x\theta} \end{Bmatrix} \tag{4}$$

where $\sigma_z = \varepsilon_z = 0$.

The equation of motion and related boundary conditions can be derived by using Hamilton's principle.The dynamic version of Hamilton's principle can be expressed as:

$$\int_{t_1}^{t_2}(\delta KE-\delta PE)dt=0 \tag{5}$$

where *KE* and *PE* are kinetic energy and potential energy, respectively. This function can be written as:

$$\begin{aligned} KE &= \frac{1}{2}\int_{-h/2}^{h/2}\int_0^{\theta}\int_{l_1}^{l_2}\rho\left[\left(\frac{\partial U}{\partial t}\right)^2+\left(\frac{\partial V}{\partial t}\right)^2+\left(\frac{\partial W}{\partial t}\right)^2\right]R(x)dxd\theta dz \\ PE_p &= \int_{-h/2}^{h/2}\int_0^{\theta}\int_{l_1}^{l_2}(\sigma_{ii}\varepsilon_{ii}+\sigma_{ij}\gamma_{ij})dxdydz\,,(i,j=x,\theta,z)i\neq j \end{aligned} \tag{6}$$

By substituting variation of kinetic and potential energy in Hamilton principle, applying side condition and by part integration, in the absence of body forces, the governing equations are as follows:

$$\begin{aligned}
&\frac{\partial N_x}{\partial x}-\frac{N_\theta}{x}+\frac{1}{x\sin\alpha}\frac{\partial N_{x\theta}}{\partial\theta}+\frac{N_x}{x}=I_1\dot{U}_0+I_2\dot{\Psi}_x+I_3\dot{\Phi}_x+I_4\dot{\eta}_x\\
&\frac{1}{x\sin\alpha}\frac{\partial N_\theta}{\partial\theta}+\frac{\cos\alpha}{x\sin\alpha}V_\theta+2\frac{N_{x\theta}}{x}+\frac{\partial N_{x\theta}}{\partial x}=I_1\dot{V}_0+I_2\dot{\Psi}_\theta+I_3\dot{\Phi}_\theta+I_4\dot{\eta}_\theta\\
&\frac{\partial V_x}{\partial x}-\frac{\cos\alpha}{x\sin\alpha}N_\theta+\frac{1}{x\sin\alpha}\frac{\partial V_\theta}{\partial\theta}+\frac{V_x}{x}=I_1\dot{W}_0\\
&\frac{\partial M_x}{\partial x}-V_x-\frac{M_\theta}{x}+\frac{1}{x\sin\alpha}\frac{\partial M_{x\theta}}{\partial\theta}+\frac{M_x}{x}=I_2\dot{U}_0+I_3\dot{\Psi}_x+I_4\dot{\Phi}_x+I_5\dot{\eta}_x\\
&\frac{1}{x\sin\alpha}\frac{\partial M_\theta}{\partial\theta}-V_\theta+\frac{\cos\alpha}{x\sin\alpha}F_\theta+2\frac{M_{x\theta}}{x}+\frac{\partial M_{x\theta}}{\partial x}=I_2\dot{V}_0+I_3\dot{\Psi}_\theta+I_4\dot{\Phi}_\theta+I_5\dot{\eta}_\theta\\
&\frac{\partial Q_x}{\partial x}-2F_x-\frac{Q_\theta}{x}+\frac{1}{x\sin\alpha}\frac{\partial Q_{x\theta}}{\partial\theta}+\frac{Q_x}{x}=I_3\dot{U}_0+I_4\dot{\Psi}_x+I_5\dot{\Phi}_x+I_6\dot{\eta}_x\\
&\frac{1}{x\sin\alpha}\frac{\partial Q_\theta}{\partial\theta}-2F_\theta+\frac{\cos\alpha}{x\sin\alpha}R_\theta+2\frac{Q_{x\theta}}{x}+\frac{\partial Q_{x\theta}}{\partial x}=I_3\dot{V}_0+I_4\dot{\Psi}_\theta+I_5\dot{\Phi}_\theta+I_6\dot{\eta}_\theta\\
&\frac{\partial P_x}{\partial x}-3R_x-\frac{P_\theta}{x}+\frac{1}{x\sin\alpha}\frac{\partial P_{x\theta}}{\partial\theta}+\frac{P_x}{x}=I_4\dot{U}_0+I_5\dot{\Psi}_x+I_6\dot{\Phi}_x+I_7\dot{\eta}_x\\
&\frac{1}{x\sin\alpha}\frac{\partial P_\theta}{\partial\theta}-3R_\theta+\frac{\cos\alpha}{x\sin\alpha}S_\theta+2\frac{P_{x\theta}}{x}+\frac{\partial P_{x\theta}}{\partial x}=I_4\dot{V}_0+I_5\dot{\Psi}_\theta+I_6\dot{\Phi}_\theta+I_7\dot{\eta}_\theta
\end{aligned} \tag{7}$$

where:

$$\begin{aligned}
&(N_i,M_i,Q_i,P_i)=\int_{-h/2}^{h/2}\sigma_i(1,z,z^2,z^3)dz \qquad i=x,\theta\\
&(N_{x\theta},M_{x\theta},Q_{x\theta},P_{x\theta})=\int_{-h/2}^{h/2}\sigma_{x\theta}(1,z,z^2,z^3)dz\\
&(V_i,F_i,R_i)=\int_{-h/2}^{h/2}\sigma_{zi}(1,z,z^2)dz \qquad i=x,\theta\\
&(S_\theta)=\int_{-h/2}^{h/2}\sigma_{z\theta}(z^3)dz\\
&(I_1,I_2,I_3,I_4,I_5,I_6,I_7)=\int_{-h/2}^{h/2}\rho(1,z,z^2,z^3,z^4,z^5,z^6)dz
\end{aligned} \tag{8}$$

Upon substituting these parameters in motion equations and obtaining motion equations in terms of displacement components, the coefficients can be expressed as:

$$\begin{bmatrix} A_{11} & B_{11} & L_{11} & q_{11} & K_{11} & T_{11} \\ A_{22} & B_{22} & L_{22} & q_{22} & K_{22} & T_{22} \\ A_{33} & B_{33} & L_{33} & q_{33} & K_{33} & T_{33} \\ A_{44} & B_{44} & L_{44} & q_{44} & K_{44} & T_{44} \\ A_{55} & B_{55} & L_{55} & q_{55} & K_{55} & T_{55} \\ A_{66} & B_{66} & L_{66} & q_{66} & K_{66} & T_{66} \\ A_{77} & B_{77} & L_{77} & q_{77} & K_{77} & T_{77} \end{bmatrix} = \int_{-\frac{h}{2}}^{\frac{h}{2}} \begin{bmatrix} 1 \\ z \\ z^2 \\ z^3 \\ z^4 \\ z^5 \\ z^6 \end{bmatrix} [C_{11} \quad C_{12} \quad C_{22} \quad C_{44} \quad C_{55} \quad C_{66}] dz \tag{9}$$

Clamped-Clamped(C-C) and Simply-Simply(S-S) boundary conditions can be described as follows:

$$\begin{aligned} &U_0 = V_0 = W_0 = \Psi_x = \Psi_\theta = \eta_x = \eta_\theta = \Phi_x = \Phi_\theta = 0 \qquad \text{Clamped supported} \\ &V_0 = W_0 = N_x = M_x = Q_x = P_x = M_{x\theta} = Q_{x\theta} = P_{x\theta} = 0 \qquad \text{Simply supported} \end{aligned} \tag{10}$$

For normal mode analysis, the following solutions may be assumed for the displacement components[28,29]:

$$\begin{aligned} U_0(x,\theta,t) &= u_0(x)\cos(m\theta)e^{i\omega t} \\ V_0(x,\theta,t) &= v_0(x)\sin(m\theta)e^{i\omega t} \\ W_0(x,\theta,t) &= w_0(x)\cos(m\theta)e^{i\omega t} \\ \eta_x(x,\theta,t) &= \eta_x(x)\cos(m\theta)e^{i\omega t} \\ \eta_\theta(x,\theta,t) &= \eta_\theta(x)\sin(m\theta)e^{i\omega t} \\ \Psi_x(x,\theta,t) &= \psi_x(x)\cos(m\theta)e^{i\omega t} \\ \Psi_\theta(x,\theta,t) &= \psi_\theta(x)\sin(m\theta)e^{i\omega t} \\ \Phi_x(x,\theta,t) &= \varphi_x(x)\cos(m\theta)e^{i\omega t} \\ \Phi_\theta(x,\theta,t) &= \varphi_\theta(x)\sin(m\theta)e^{i\omega t} \end{aligned} \tag{11}$$

where "*m*" is circumferential wave number respectively, and w is the natural angular frequency of the vibration. The truncated conical has continuouly graded fiber volume fraction through the thickness direction. In the present analysis, it is assumed that fiber angle of the fiber reinforced truncated conical shell is constant with respect to the *x*-axis in the $x-\theta$ surface. The effective mechanical properties of the fiber reinforced truncated conical shell are obtained based on a micromechanical model as follows (Vasiliev and Morozov [30]):

$$\begin{aligned} E_1 &= V_f E_1^f + V_m E_1^m \\ \frac{1}{E_2} &= \frac{V_f}{E_2^f} + \frac{V_m}{E_2^m} - V_f V_m \frac{\upsilon_f^2 E_2^m / E_2^f + \upsilon_m^2 E_2^f / E_2^m - 2\upsilon^f \upsilon^m}{V_f E_2^f + V_m E_2^m} \\ \frac{1}{G_{ij}} &= \frac{V_f}{G_{ij}^f} + \frac{V_m}{G_{ij}^m} (ij = 12,13,23) \\ \upsilon_{12} &= V_f \upsilon^f + V_m \upsilon^m \\ \rho &= V_f \rho^f + V_m \rho^m \end{aligned} \tag{12}$$

where $E_{ii}^f, G_{ij}^f, \upsilon^f$ and ρ^f are elasticity modulus, shear modulus, Poisson's ratio and density of the fiber, and $E_{ii}^m, G_{ii}^m, \upsilon^m$ and ρ^m are corresponding properties for the matrix. V_f and V_m are the fiber and matrix volume fractions respectively and are related by $V_f + V_m = 1$.

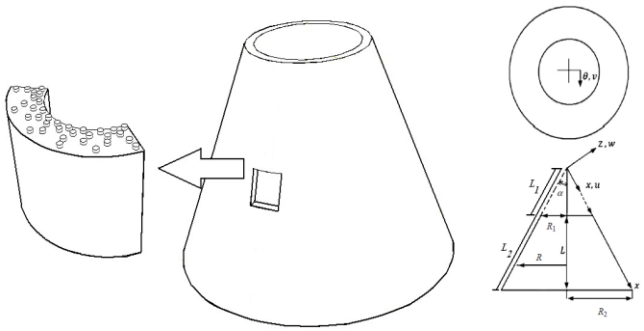

Fig.1
Conical shell coordinate system.

In this case, the volume fraction of the fibers has continuous variations in the thickness direction. Two models for fiber volume fractions variations in the thickness direction are considered which are described as follows:

The first model is according to Eq. (13). For even power (*P*), fibers volume fraction variations are symmetric:

$$V = V_i \left(\frac{2z}{h}\right)^P + V_o \tag{13}$$

where V_i and V_o which have values that range from 0 to 1, denote the volume fractions (matrix or fiber) on the inner and outer surfaces, respectively. The exponent P controls the volume fraction profile through the shell's thickness.

According to symmetrical model, changes in fiber`s volume fraction occur from 0.75 on internal surface $(z = -h/2)$ to 0 at mid-surface, and again reach to 0.75 in periphery $z = h/2$ of the cone. The symmetrical distribution of fibers` volume fraction along thickness of the cone is shown in Fig. 2. As observed in Fig. 2 , the variations tend toward 0% volume fraction of fiber throughout the thickness of the cone for large values of even power indices, which are similar to a homogenous orthotropic cone with 0% volume fraction of fiber and 100% matrix throughout thickness. Non dimensional parameter $\eta = z/h$ is introduced for thickness of the cone.

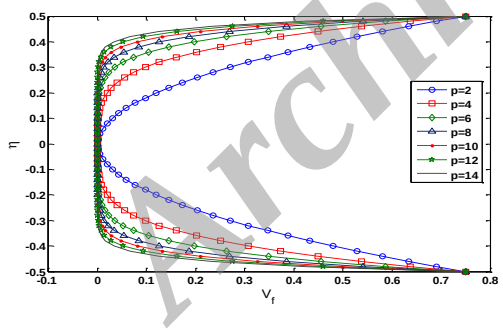

Fig.2
Symmetric variations of fibers volume fractions through the thickness for functionally orthotropic truncated conical shell according to Eq. (13).

The second model is according to Eq. (14) which is called the classical model:

$$V = (V_i - V_o)\left(\frac{z}{h} + \frac{1}{2}\right)^P + V_o \tag{14}$$

Based on Classical model, fibers` volume fraction reaches to 0.75 in periphery from zero on internal surface of truncated cone continuously. According to this relation, V_i and V_o which have values that range from 0 to 1, denote the volume fractions (matrix or fiber) on the inner and outer surfaces, respectively. Fig. 3 illustrates this distribution per different power indices. According to this Figure fibers volume fraction is zero in $(z = -h/2)$ and 0.75 in $z = h/2$.

The variations tend toward 0% volume fraction of fiber for large values of power indices, which is similar to a homogenous orthotropic cone with 0% of fibers and 100% of the matrix volume fraction throughout the cone thickness.

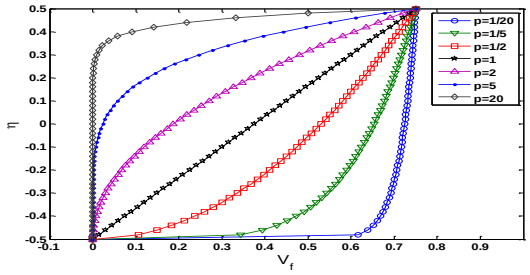

Fig.3
Classic variations of fibers volume fractions through the thickness for functionally graded orthotropic truncated conical shell according to Eq. (14).

3 SOLUTION PROCEDURE

At this stage, the transversely discretized governing differential equations and the related boundary conditions are transformed into the algebraic equations via the GDQ method.

It is difficult to solve the equations of motion analytically, if it could not be possible. Hence, one should use a semi-analytical or numerical method to find a solution. Differential quadrature method (DQM) is applied to solve the equations in this literature.

The essence of the differential quadrature method is that the partial derivative of a function, with respect to a space variable at a given sampling point, is approximated as a weighted linear sum of the discrete points in the desire direction. In order to show the DQ estimation, consider a smooth function $f(\xi)$ having its field on a domain 0<x<a. Let in the given domain the function values be known or desired on a grid of sampling points. According to DQ method, for higher order derivatives of the function $f(\xi)$ can be expressed by one recursion formula (Bert and Malik [31]):

$$\frac{\partial^m f(\xi_i)}{\partial \xi^m} = \sum_{n=1}^{N_\xi} A_{in}^{\xi(m)} f_n \qquad for\ i = 1,2,...,N_\xi \tag{15}$$

where the superscript m, denote the order of the derivative.

From this equation, one can perceive that the weighting coefficients $A_{in}^{\xi(m)}$ and the select of sampling points are the essential components of DQ approximations. In order to obtain the weighting coefficients, a set of test functions should be employed in Eq. (15). For polynomial basis functions DQ, a set of Lagrange polynomials are employed as test functions. The weighting coefficients for the first-order derivatives in ξ_i-direction are thus achieved as (Bert and Malik [31]):

$$A_{in}^{\xi} = \begin{cases} \dfrac{1}{L_\xi} \dfrac{M(\xi_i)}{(\xi_i - \xi_j) M(\xi_j)} & for\ i \neq j \\ -\sum\limits_{\substack{j=1 \\ i \neq j}}^{N_\xi} A_{in}^{\xi} & for\ i = j; \quad i, j = 1,2,....,N_\xi \end{cases} \tag{16}$$

where

$$M(\xi_i) = \prod_{j=1, i \neq j}^{N_\xi} (\xi_i - \xi_j) \tag{17}$$

The weighting coefficients of the second-order derivative can be obtained as (Bert and Malik [31]):

$$[B_{in}^{\xi}]=[A_{in}^{\xi}][A_{in}^{\xi}]=[A_{in}^{\xi}]^2 \tag{18}$$

Eq. (18) being applied to Eqs. (15)- (17), equations of motion (7) based on displacement field by GDQ method are discretized as Appendix A.That i=2,…, N-1. Hence, for Clamped-Clamped (C-C) boundary conditions:

$$u_{0i}=v_{0i}=w_{0i}=\psi_{xi}=\psi_{\theta i}=\phi_{xi}=\phi_{\theta i}=\eta_{xi}=\eta_{\theta i}=0\,, \qquad i=1,N \tag{19}$$

and for Simply-Simply(S-S) boundary conditions at the both ends of the truncated conical shell is discretized as Appendix A:

In order to carry out the eigenvalue analysis, the domain and boundary degrees of freedom are separated and in vector forms. They are denoted as {d} and {b}, respectively. Based on this definition, the discretized form of the motion equations and the related boundary conditions take the following forms:

Equations of motion (Appendix A (1-9)):

$$[[K_{db}] \quad [K_{dd}]]\begin{Bmatrix}\{b\}\\ \{d\}\end{Bmatrix}-\omega^2[M]\{d\}=\{0\} \tag{20}$$

Boundary conditions (Eqs. (19) or Appendix A (10)):

$$[K_{bd}]\{d\}+[K_{bb}]\{b\}=\{0\} \tag{21}$$

By eliminating the boundary degrees of freedom in Eq. (20), using Eq. (21), this equation turn into:

$$([K]-\omega^2[M])\{d\}=\{0\} \tag{22}$$

where $[K]=[K_{dd}]-[K_{db}][K_{bb}]^{-1}[K_{bd}]$. The above eigenvalue system of equations can be solved to find the natural frequencies and mode shapes of the orthotropic CG truncated conical shell.

4 RESULTS AND DISCUSSION

4.1 Verification of the results

There is a comparison in the form of some examples to validate the derived equations and applied numerical method. In Table 1. comparison has been made between the present results which are based on third-order theory by GDQM and FEM for the first three natural frequencies of isotropic CG truncated conical shell with Clamped - Clamped boundary condition. In this table the results are presented for different power index as well as the radius to thickness ratio. As noticed there is good agreement between the results.

The effective material properties of the isotropic CG shell are assumed to vary as follows:

$$\begin{aligned}&E(z)=(E_m-E_c)(z/h+0.5)^P+E_c\\ &\rho(z)=(\rho_m-\rho_c)(z/h+0.5)^P+\rho_c\\ &E_m=70GPa, E_c=380GPa\\ &\rho_m=2702\frac{kg}{m^3},\ \rho_c=3800\frac{kg}{m^3}\\ &v=0.3\end{aligned} \tag{23}$$

Further comparisons were made with the references Liew [22], and Irie et al. [32] for the homogenous isotropic truncated conical shell in Tables 2-3. In reference [22] analysis is carried out using the element-free kp-Ritz method. This method is developed based on the kernel particle concept; the hybrid displacement field is approximated by the product of kernel particle (kp) functions in the longitudinal direction, and harmonic functions in the circumferential

direction. By combining the kernel particle concept with the Ritz procedure, eigenequations for the free vibration of conical shells are derived. Study is based on the classical thin-shell theory. Also in reference [32] the natural frequencies are obtained for truncated conical shells of uniform thickness under nine combinations of boundary conditions. In the both references formulation is based on a classical thin-shell theory. The results for values of circumferential wave number and different angles of the cone are presented.

The comparison shows that the present results agree well with those in the literatures and it is observed there is good agreement between the results.

Table 1
Comparison of dimensionless natural frequency of isotropic CG truncated conical shell with (C-C) boundary condition ($L / R_2 = 1,\ \Omega = \omega h\sqrt{\rho_m / E_m},\ \alpha = 30^0$).

		p=0		p=0.5		p=1		p=5	
R_2 / h		Present	FEM	Present	FEM	Present	FEM	Present	FEM
5	m=0	0.3173	0.3174	0.4591	0.4616	0.5047	0.5014	0.5830	0.5864
	m=1	0.2782	0.2777	0.4028	0.4069	0.4423	0.4457	0.5108	0.5100
	m=2	0.2689	0.2677	0.3887	0.3946	0.4253	0.4301	0.4914	0.4908
10	m=0	0.1330	0.1330	0.1942	0.1965	0.2137	0.2160	0.2453	0.2468
	m=1	0.1124	0.1124	0.1639	0.1650	0.1801	0.1812	0.2067	0.2073
	m=2	0.0973	0.0971	0.1408	0.1418	0.1539	0.1547	0.1767	0.1769

Table 2
Comparison of dimensionless natural frequency of isotropic truncated conical shell with (C-C) boundary conditions ($h / R_2 = 0.01,\ L\sin(\alpha) / R_2 = 0.5,\ \Omega = \omega R_2\sqrt{\rho(1-\nu^2) / E}$).

	$\alpha = 30^0$		$\alpha = 45^0$			$\alpha = 60^0$	
m	Present	Irie [32]	Present	Irie [32]	Liew [22]	Present	Irie [32]
0	0.9925	0.9930	0.8726	0.8731	0.8732	0.6682	0.6685
1	0.8775	0.8776	0.8117	0.8120	0.8120	0.6313	0.6316
2	0.6420	0.6422	0.6694	0.6696	0.6696	0.5520	0.5523
3	0.4799	0.4803	0.5426	0.5430	0.5428	0.4780	0.4785
4	0.3808	0.3816	0.4563	0.4570	0.4565	0.4290	0.4298
5	0.3299	0.3311	0.4085	0.4095	0.4088	0.4083	0.4093
6	0.3200	0.3216	0.3956	0.3970	0.3961	0.4145	0.4159
7	0.3429	0.3450	0.4133	0.4151	0.4141	0.4448	0.4466
8	0.3883	0.3906	0.4555	0.4577	0.4567	0.4950	0.4972
9	0.4478	0.4505	0.5159	0.5186	0.5175	0.5612	0.5640

Table 3
Comparison of dimensionless natural frequency of isotropic truncated conical shell with (S-S) boundary conditions ($h / R_2 = 0.01,\ L\sin(\alpha) / R_2 = 0.5,\ \Omega = \omega R_2\sqrt{\rho(1-\nu^2) / E}$).

	$\alpha = 30^0$		$\alpha = 45^0$			$\alpha = 60^0$	
m	Present	Irie [32]	Present	Irie [32]	Liew [22]	Present	Irie [32]
0	0.1524	0.1527	0.2230	0.2233	0.2234	0.2348	0.2350
1	0.6506	0.6567	0.5419	0.5462	0.5462	0.4040	0.4065
2	0.6116	0.6189	0.6263	0.6310	0.6309	0.4796	0.4821
3	0.4106	0.4157	0.5005	0.5065	0.5061	0.4276	0.4317
4	0.2955	0.2988	0.3899	0.3947	0.3941	0.3645	0.3687
5	0.2507	0.2535	0.3310	0.3348	0.3337	0.3322	0.3359
6	0.2583	0.2612	0.3215	0.3248	0.3235	0.3368	0.3402
7	0.2966	0.2996	0.3491	0.3524	0.3510	0.3716	0.3748
8	0.3497	0.3529	0.3998	0.4033	0.4019	0.4270	0.4305
9	0.4115	0.4152	0.4645	0.4684	0.4671	0.4964	0.5004

4.2 Convergence

The rate of convergence is investigated in Table 4. for various geometric parameters. As one can observe fast rate of convergence of the method is quite eviden and it is found only 11 grid points in the thickness direction can yield accurate results.

Table 4
Rate of convergence for the first three non-dimensional natural frequencies in terms of (C-C) boundary condition for CG truncated conical shell classic distribution of fiber $(L/R_2=1$, $\Omega=\omega R_2\sqrt{\rho_m(1-v_m^2)/E_m}$,p=1) .

R_2/h	α		N=5	N=7	N=9	N=11	N=13	N=15
10	30	m=0	1.2984	1.2944	1.2940	1.2940	1.2940	1.2940
		m=1	1.0884	1.0922	1.0920	1.0920	1.0921	1.0921
		m=2	0.9432	0.9525	0.9521	0.9522	0.9522	0.9522
	60	m=0	1.0362	1.0545	1.0521	1.0521	1.0522	1.0522
		m=1	0.8907	0.9251	0.9222	0.9223	0.9223	0.9223
		m=2	0.9050	0.9345	0.9313	0.9314	0.9314	0.9314
20	30	m=0	1.1806	1.1621	1.1586	1.1585	1.1585	1.1585
		m=1	0.9540	0.9554	0.9543	0.9543	0.9543	0.9543
		m=2	0.7388	0.7478	0.7472	0.7472	0.7472	0.7472
	60	m=0	0.9001	0.8832	0.8773	0.8773	0.8773	0.8773
		m=1	0.7229	0.7414	0.7364	0.7364	0.7364	0.7364
		m=2	0.5967	0.6270	0.6220	0.6219	0.6219	0.6219

The results related to free vibration of CG fiber reinforced truncated conical shell are presented for two different symmetric and classic distributions. For this purpose dimensionless parameter $\Omega=\omega R_2\sqrt{\rho_m(1-v_m^2)/E_m}$ is used for the natural frequency ω which υ_m, E_m, ρ_m are Poisson`s ratio, Young`s modulus and density respectively. In this paper, Tungsten and Copper are used as fiber and matrix, respectively which their material properties are given in Table 5.

Table 5
Mechanical properties of the fiber and matrix.

	E (GPa)	$\rho(kg/m^3)$	v
Copper	115	8960	0.31
Tungsten	400	19300	0.28

As observed in Figs. 4(a)-(c) , the first three natural frequencies decrease with the increase of fibers volume fraction power versus volume fraction power for both classic and symmetric fibers distributions. The obtained natural frequency values for symmetrical distribution of fibers volume fraction are more than natural frequency values for classic distribution. This just occurs in a special range of volume fraction index for symmetrical distribution. But, the resulting natural frequencies from both distribution of fibers volume fraction are equal for large values of fiber volume fraction power. That is because of the fibers volume fraction tends toward zero throughout the thickness of truncated conical shell with the increase of power and only 100% of matrix is remained as demonstrated in Figs. 2 and 3.

It shows that non-dimensional natural frequency tends to constant values for larger values of the volume fraction power.

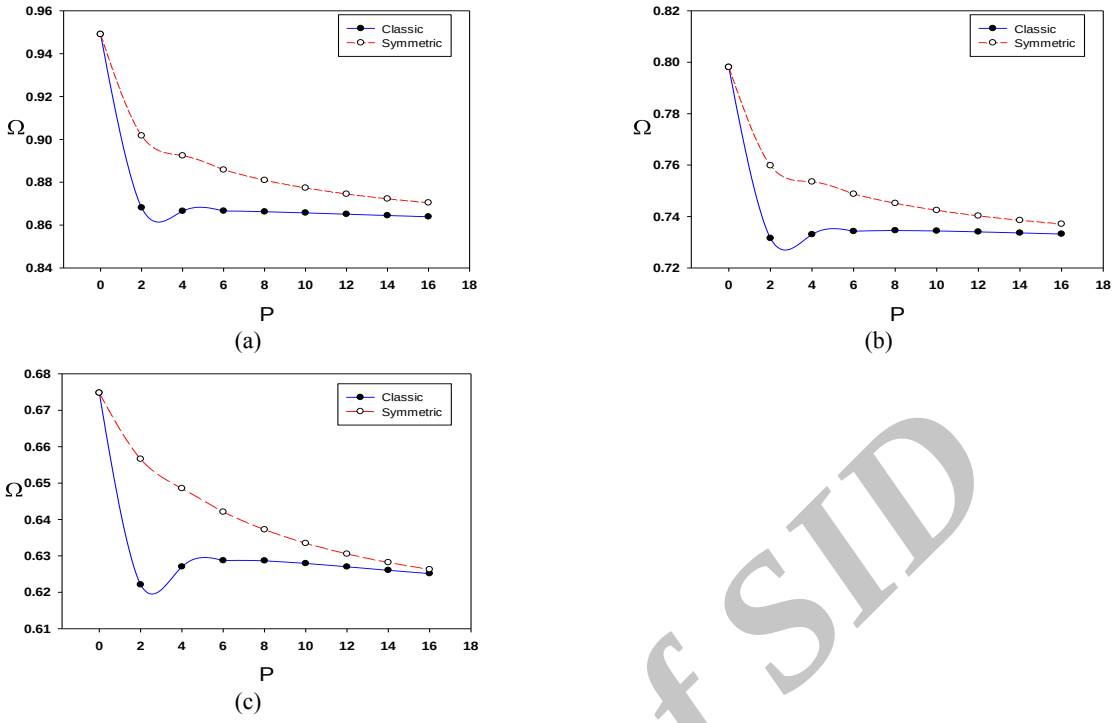

Fig.4
Comparison of the first three non-dimensional frequencies variations versus volume fraction index for CGFR with classic and symmetric fibers distribution, (a) m=0, (b) m=1, (c) m=2, $(L/R_2=1, R_2/h=20, \alpha=60\ , C-C)$.

In fact, the orthotropic CG truncated conical shell is approached to a homogenous orthotropic truncated conical shell for larger power values. This case can be clearly seen in Figs. 5(a)-(c) and 6(a)-(c) for the first three frequencies of classic and symmetric distributions in truncated conical shell for zero power ($P=0$) which are the demonstrator of an orthotropic homogenous truncated conical shell with 75% fiber and 25% matrix, infinite power($P=\infty$) which indicates an orthotropic homogenous truncated conical shell with 0% fiber and 100% matrix, and different power values of fibers volume fraction for orthotropic CG truncated conical shell through the thickness direction.

Figs. 5(a)-(c) and 6(a)-(c) show that the natural frequencies of orthotropic CG fiber reinforced truncated conical shell tend toward the natural frequencies of the orthotropic homogenous truncated conical shell with 0.75 fiber and 0.25 matrix for small power values, and also tend toward the natural frequencies of orthotropic homogenous truncated conical shell with 0% fibers and 100% matrix for large power values.

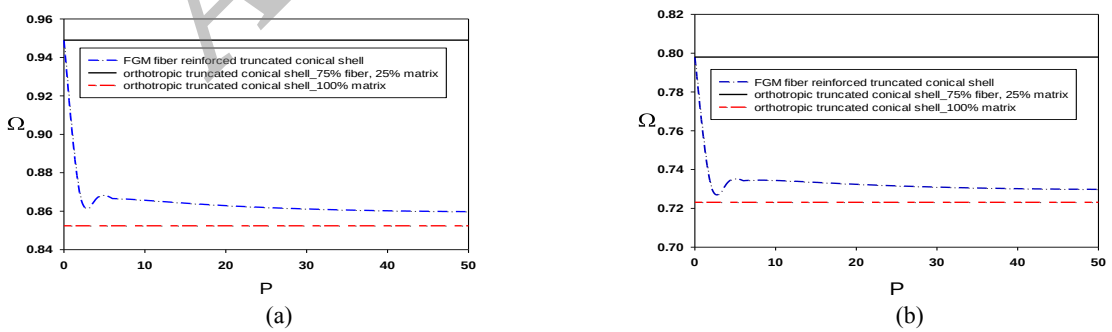

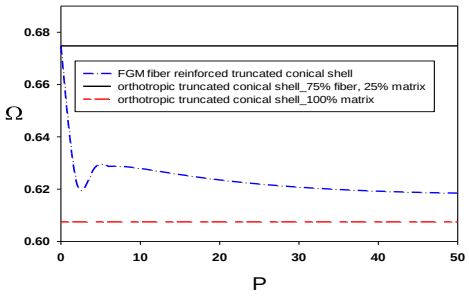

(c)

Fig.5

Variations of CGM fiber reinforced truncated conical shell in comparison with orthotropic truncated conical shell versus volume fraction power for classic distribution, (a) m=0, (b) m=1, (c) m=2, ($L/R_2=1,\ R_2/h=20,\alpha=60,C-C$).

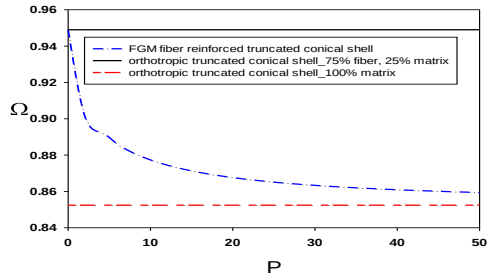

(a)

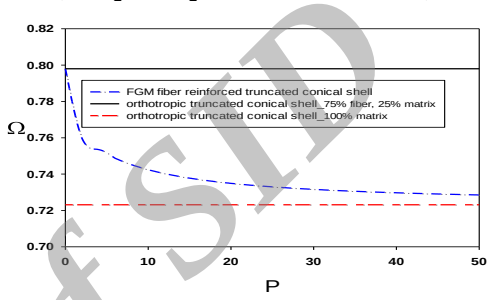

(b)

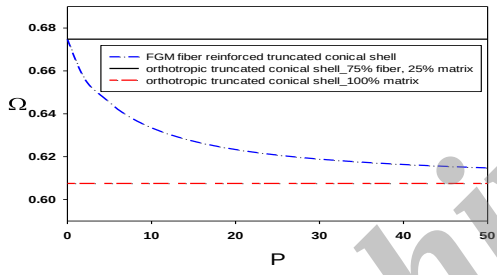

(c)

Fig.6

Variations of CGM fiber reinforced truncated conical shell in comparison with orthotropic truncated conical shell versus volume fraction power for symmetrical distribution, (a) m=0, (b) m=1, (c) m=2, ($L/R_2=1,\ R_2/h=20,m=2,\alpha=60,C-C$).

In Figs. 7(a)-(c), we characterize the vibration response of CG fiber reinforced truncated conical shell against values of large radius to thickness ratio for symmetric distribution of fibers at different values of semi-vertex angle. As expected non-dimensional natural frequency decreases with the increase of radius to thickness ratio. Also decrease of first three natural frequency are observed for symmetrical distribution by increasing semi-vertex angle of truncated cone at constant large radius to thickness ratio.

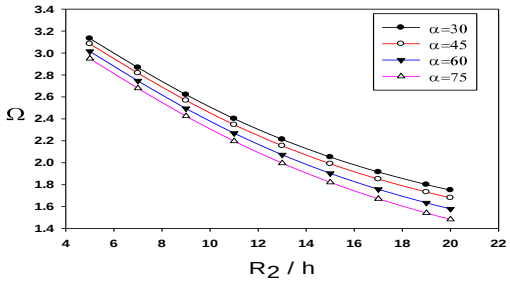

(a)

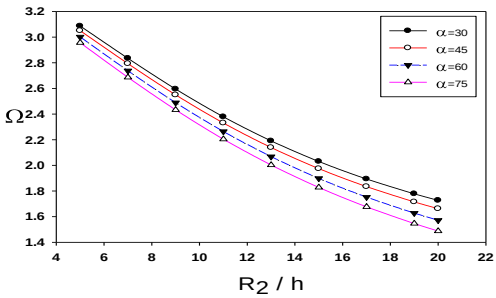

(b)

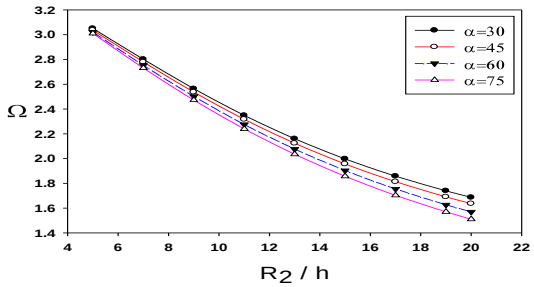

(c)

Fig.7
Variations of first three non-dimensional natural frequency versus lager radius to thickness ratio for symmetrical distribution of fibers in CGM, (a) m=0, (b) m=1, (c) m=2, $(L/R_2=0.5, P=2, C-C)$.

Figs. 8(a)-(c) demonstrates variations of first three non-dimensional natural frequency against frustum`s semi-vertex angle from zero degree ,which make the cone transformed to cylinder, up to 90 degrees, which is transmuted to annular plate, for two different powers volume fraction (0 and 6). Zero power converts the geometry to a homogenous orthotropic truncated conical shell, but non-zero power of material changes to orthotropic CGM, in which fibers volume fraction changes continuously along the thickness. In this figure, by increasing the semi-vertex angle of truncated conical shell, slight increase and then sever decrease of natural frequency is observed. The higher and lower rate of natural frequency are assigned to 30 degrees and 90 degrees, which are transmuted to an annular plate, respectively. Also, as observed, the natural frequency of homogenous orthotropic truncated conical shell is higher than that of CGFR.

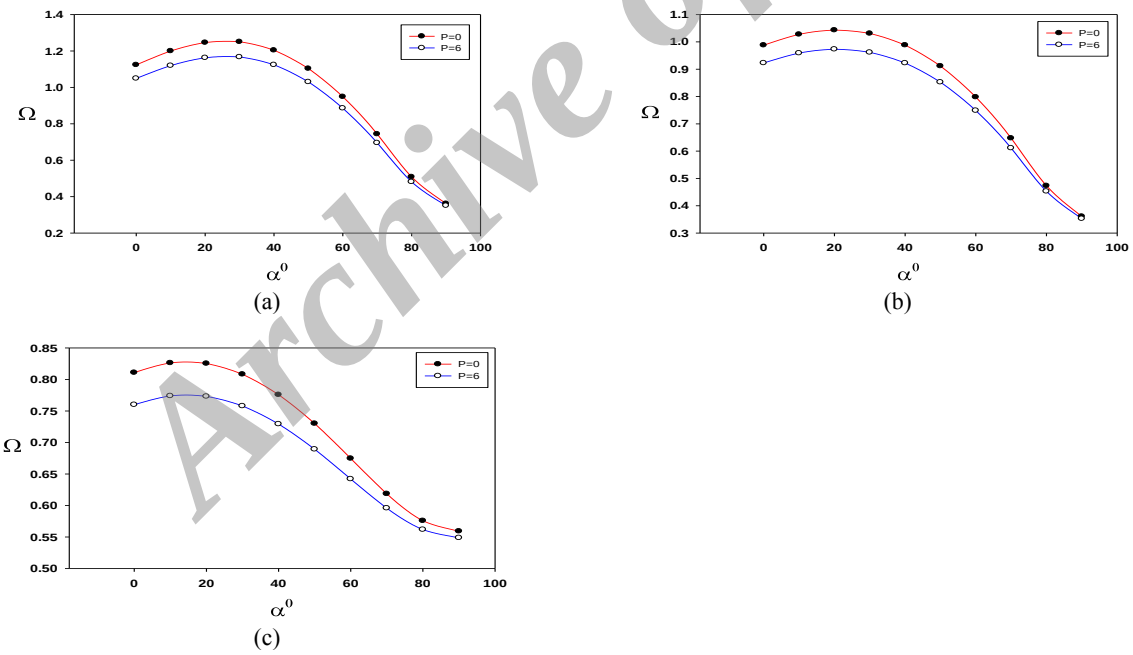

(a) (b)

(c)

Fig.8
Variations of first three non-dimensional natural frequency versus semi-vertex for symmetrical distribution of fibers in CGM, (a) m=0, (b) m=1, (c) m=2, $(L/R_2=1,\quad R_2/h=20,\quad ,C-C)$.

Variations of first three natural frequencies of CGFR shell against S rtio, which are defined as $L\sin\alpha/R_2$, are illustrated for different semi-vertex angle values in Figs. 9(a)-(c).

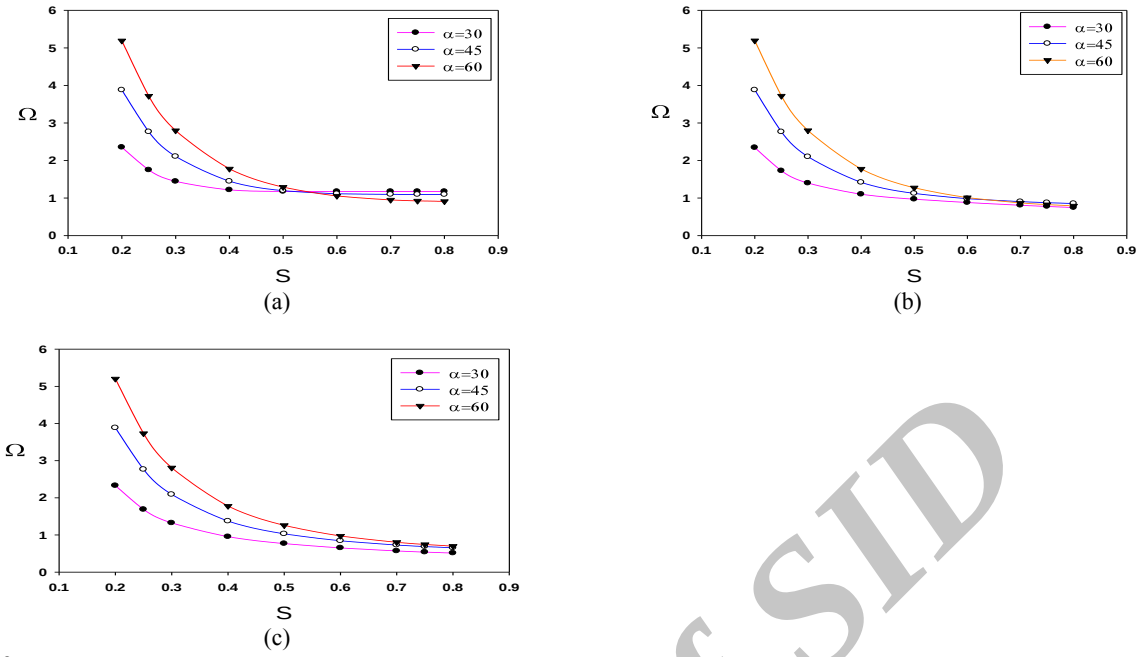

Fig.9
Variations of first three non-dimensional frequency CG fiber reinforced with classic distribution versus parameter s for different values of semi-vertex angle, (a) m=0, (b) m=1, (c) m=2, ($R_2 / h = 20, p = 2$,$C-C$).

Figs. 10(a)-(b) is plots of non-dimensional natural frequency versus circumferential wave number for different values of volume fraction power and semi-vertex angle. It is observed that, generally non-dimensional natural frequency increases. In this figure, reduction of natural frequency occures for wave number less than 3, and then increases for greater wave number. These figures are shown for different fibers volume fraction through the thickness, and also semi vertex angle parameters. This case happens for both distributions.

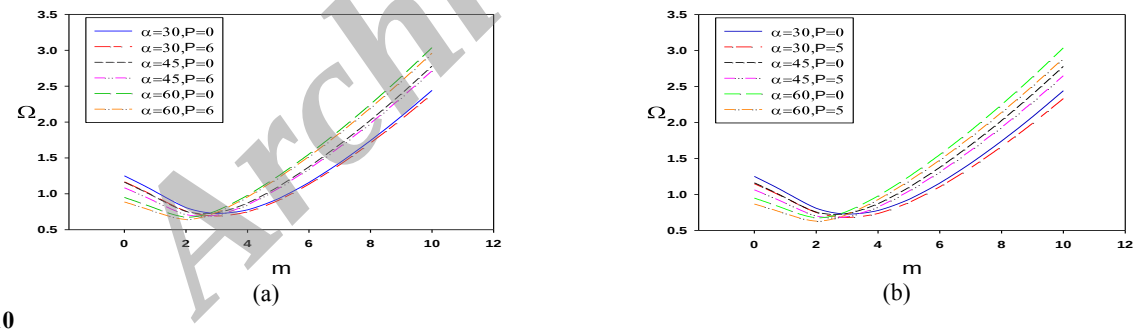

Fig.10
Variations of first non-dimensional natural frequency versus circumferential wave number for different distributions of fibers in CGM, (a) Symmetric, (b) Classic, ($L / R_2 = 1, R_2 / h = 20, C-C$) .

Figs.11(a)-(b) shows comparison between orthotropic CGFR and composite multi-layers truncated conical shells. In this analogy, results of a composite truncated conical shell with 3 and 5 layers are presented in which the volume fraction ratio of fiber to matrix is different in each layer according to Table 6.

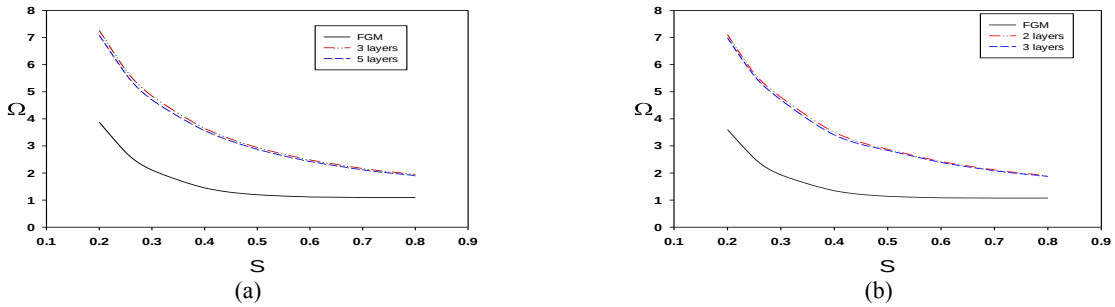

Fig.11
Comparison of first non-dimensional frequency CG fiber reinforced with a Symmetric distribution and multi-layer,(a) Symmetric(P=2), (b) Classic(P=1) ($R_2/h=20,\ \alpha=45, m=0, C-C$).

Table 6
Material volume fractions of 3-layer, 5-layer and fiber reinforced FGM.

		Type of distribution	
Type of truncated conical shell		Symmetric distribution	Classic distribution
3 layers	First layer	75% Fiber, 25% Matrix	0% Fiber, 100% Matrix
	Second layer	0% Fiber, 100% Matrix	37.5% Fiber, 62.5% Matrix
	Third layer	75% Fiber, 25% Matrix	75% Fiber, 25% Matrix
5 layers	First layer	75% Fiber, 25% Matrix	0% Fiber, 100% Matrix
	Second layer	37.5% Fiber, 62.5% Matrix	18.75% Fiber, 81.25% Matrix
	Third layer	0% Fiber, 100% Matrix	37.5% Fiber, 62.5% Matrix
	Forth layer	37.5% Fiber, 62.5% Matrix	56.25% Fiber, 43.75% Matrix
	Fifth layer	75% Fiber, 25% Matrix	75% Fiber, 25% Matrix
Fiber rein forced FGM	Inner surface	75% Fiber, 25% Matrix	0% Fiber, 100% Matrix
	Outer surface	75% Fiber, 25% Matrix	75% Fiber, 25% Matrix

The natural frequency of orthotropic continuously graded fiber reinforced truncated conical shell is much smaller than multilayer composite for small values of *S* ratios. This difference becomes less for larger values of *S* ratios. Although it is observed that the natural frequency of composite truncated conical shell is inclined to orthotropic CGFR truncated conical shell with increasing layers in composite truncated conical shell, it will be equaled with high number of layers.

Tables 7-8., show the first to fourth non-dimensional frequency at different semi-vertex angles, volume fraction power and greater radius to thickness ratio for two different distributions of symmetric and classic fibers volume fractions through the thickness of truncated conical shell.

Table 7
First to forth non-dimensional natural frequencies for symmetric distribution and S-S boundary condition ($L/R_2=1$).

		$R_2/h=10$			$R_2/h=20$		
		P=2	P=6	P=10	P=2	P=6	P=10
$\alpha=30$	m=0	0.28907	0.283139	0.280188	0.240689	0.236572	0.234536
	m=1	0.716776	0.7132	0.711668	0.684675	0.682438	0.681856
	m=2	0.759657	0.749933	0.744743	0.652537	0.648931	0.647438
	m=3	0.810414	0.79363	0.784079	0.555835	0.545883	0.540797
$\alpha=60$	m=0	0.485535	0.472557	0.464862	0.380249	0.37174	0.367408
	m=1	0.663694	0.651739	0.644827	0.554365	0.547101	0.543374
	m=2	0.753739	0.738385	0.729152	0.523671	0.516385	0.512395
	m=3	1.055988	1.032326	1.017193	0.614513	0.600143	0.591489
$\alpha=75$	m=0	0.473237	0.459266	0.449059	0.319331	0.309539	0.303907
	m=1	0.539492	0.522997	0.512969	0.374284	0.366454	0.36185
	m=2	0.782706	0.761759	0.748233	0.453693	0.442407	0.435457
	m=3	1.146109	1.118988	1.100975	0.630357	0.612773	0.601727

Table 8
First to forth non-dimensional natural frequencies for classic distribution and S-S boundary condition (L/R_2=1).

		$R_2/h=10$			$R_2/h=20$		
		P=1	P=5	P=10	P=1	P=5	P=10
$\alpha=30$	m=0	0.281444	0.280588	0.280282	0.236364	0.235518	0.234943
	m=1	0.71062	0.704412	0.706152	0.684437	0.678117	0.679115
	m=2	0.745926	0.750754	0.749165	0.650596	0.649511	0.649017
	m=3	0.774372	0.790829	0.78826	0.541634	0.545716	0.542858
$\alpha=60$	m=0	0.459969	0.454397	0.454508	0.369439	0.363599	0.362844
	m=1	0.632146	0.628295	0.629851	0.542928	0.536587	0.536653
	m=2	0.716244	0.729192	0.72815	0.508388	0.512272	0.511536
	m=3	0.983089	1.010068	1.010181	0.573843	0.587654	0.586494
$\alpha=75$	m=0	0.434473	0.433752	0.434406	0.302044	0.296917	0.29599
	m=1	0.486569	0.490122	0.490714	0.354377	0.353248	0.353424
	m=2	0.720835	0.738188	0.738032	0.421889	0.429945	0.429474
	m=3	1.058898	1.088337	1.08935	0.577476	0.594102	0.593201

5 CONCLUSIONS

In this study, free vibrations of CGFR throughout the thickness of truncated conical shell are investigated. The governing equations of motion for orthotropic CG conical shell based on TSDT are derived and solved by GDQ method which has the higher accuracy and convergence rate. Two different types of fiber distributions through the thickness including symmetric and classic profiles are considered and compared with each-other.
From this study some conclusions are made as follows:

Decrease of first three non-dimensional natural frequencies with the increase of fibers volume fraction power for both symmetric and classic profiles of fibers volume fraction at constant R_2/h and L/R_2.

The non-dimensional natural frequency of symmetric distribution is larger than classic one for specific volume fraction power.

The non-dimensional natural frequency decreased by increasing the greater radius to thickness ratio.

The natural frequency decreased by increasing the semi-vertex angle of truncated conical shell which gets close to the geometry of annular plate at constant R_2/h and L/R_2.

The non-dimensional natural frequency of the laminated composite is greater than similar orthotropic CG truncated conical shell. There is a large difference between non-dimensional natural frequency values of orthotropic CG truncated conical shell and laminated composite. This difference becomes less with increasing the layers of the laminated composite one.

APPENDIX A

Equations of motion (7) based on displacement field by GDQ method are discretized as:

$$
\begin{aligned}
&-\left(\frac{L_{11}}{x^2}+\frac{m^2T_{11}}{x^2\sin^2\alpha}\right)u_{0i}-\left(\frac{mL_{11}}{x^2\sin\alpha}+\frac{mT_{11}}{x^2\sin\alpha}\right)v_{0i}+\left(-\frac{L_{11}\cos\alpha}{x^2\sin\alpha}\right)w_{0i}-\left(\frac{L_{22}}{x^2}+\frac{m^2T_{22}}{x^2\sin^2\alpha}\right)\psi_{xi}-\left(\frac{mL_{22}}{x^2\sin\alpha}+\frac{mT_{22}}{x^2\sin\alpha}\right)\psi_{\theta i}\\
&-\left(\frac{L_{33}}{x^2}+\frac{m^2T_{33}}{x^2\sin^2\alpha}\right)\phi_{xi}-\left(\frac{mL_{33}}{x^2\sin\alpha}+\frac{mT_{33}}{x^2\sin\alpha}\right)\phi_{\theta i}-\left(\frac{L_{44}}{x^2}+\frac{m^2T_{44}}{x^2\sin^2\alpha}\right)\eta_{xi}-\left(\frac{mL_{44}}{x^2\sin\alpha}+\frac{mT_{44}}{x^2\sin\alpha}\right)\eta_{\theta i}+\\
&\sum_{j=1}^{N}\left(\frac{A_{11}}{x}c_{ij}^{(1)}+A_{11}c_{ij}^{(2)}\right)u_{0j}+\left(\frac{m}{x\sin\alpha}\right)\sum_{j=1}^{N}c_{ij}^{(1)}(T_{11}+B_{11})v_{0j}+\sum_{j=1}^{N}c_{ij}^{(1)}\left(\frac{B_{11}\cos\alpha}{x\sin\alpha}\right)w_{0j}+\sum_{j=1}^{N}\left(\frac{A_{22}}{x}c_{ij}^{(1)}+A_{22}c_{ij}^{(2)}\right)\psi_{xj}\\
&+\left(\frac{m}{x\sin\alpha}\right)\sum_{j=1}^{N}c_{ij}^{(1)}(T_{22}+B_{22})\psi_{\theta j}+\sum_{j=1}^{N}\left(\frac{A_{33}}{x}c_{ij}^{(1)}+A_{33}c_{ij}^{(2)}\right)\phi_{xj}+\left(\frac{m}{x\sin\alpha}\right)\sum_{j=1}^{N}c_{ij}^{(1)}(T_{33}+B_{33})\phi_{\theta j}+\sum_{j=1}^{N}\left(\frac{A_{44}}{x}c_{ij}^{(1)}+A_{44}c_{ij}^{(2)}\right)\eta_{xj}\\
&+\left(\frac{m}{x\sin\alpha}\right)\sum_{j=1}^{N}c_{ij}^{(1)}(T_{44}+B_{44})\eta_{\theta j}=-\omega^2(I_1u_{0i}+I_2\psi_{xi}+I_3\phi_{xi}+I_4\eta_{xi})
\end{aligned}
\qquad (A.1)
$$

$$
\begin{aligned}
&-\left(\frac{mL_{11}}{x^2\sin\alpha}+\frac{mT_{11}}{x^2\sin\alpha}\right)u_{0i}+(-\frac{m^2L_{11}}{x^2\sin^2\alpha}-\frac{T_{11}}{x^2}-\frac{q_{11}\cos^2\alpha}{x^2\sin^2\alpha})v_{0i}-(\frac{mL_{11}\cos\alpha}{x^2\sin^2\alpha}+\frac{mq_{11}\cos\alpha}{x^2\sin^2\alpha})w_{0i}\\
&-(\frac{mL_{22}}{x^2\sin\alpha}+\frac{mT_{22}}{x^2\sin\alpha})\psi_{xi}+(-\frac{m^2L_{22}}{x^2\sin^2\alpha}-\frac{T_{22}}{x^2}+\frac{q_{11}\cos\alpha}{x\sin\alpha}-\frac{q_{22}\cos^2\alpha}{x^2\sin^2\alpha})\psi_{\theta i}-(\frac{mL_{33}}{x^2\sin\alpha}+\frac{mT_{33}}{x^2\sin\alpha})\phi_{xi}+\\
&(-\frac{m^2L_{33}}{x^2\sin^2\alpha}-\frac{T_{33}}{x^2}+\frac{2q_{22}\cos\alpha}{x\sin\alpha}-\frac{q_{33}\cos^2\alpha}{x^2\sin^2\alpha})\phi_{\theta i}-(\frac{mL_{44}}{x^2\sin\alpha}+\frac{mT_{44}}{x^2\sin\alpha})\eta_{xi}+\\
&(-\frac{m^2L_{44}}{x^2\sin^2\alpha}-\frac{T_{44}}{x^2}+\frac{3q_{33}\cos\alpha}{x\sin\alpha}-\frac{q_{44}\cos^2\alpha}{x^2\sin^2\alpha})\eta_{\theta i}-(\frac{m}{x\sin\alpha})\sum_{j=1}^{N}c_{ij}^{(1)}(T_{11}+B_{11})u_{0j}+\sum_{j=1}^{N}(\frac{T_{11}}{x}c_{ij}^{(1)}+T_{11}c_{ij}^{(2)})v_{0j}\\
&-(\frac{m}{x\sin\alpha})\sum_{j=1}^{N}c_{ij}^{(1)}(T_{22}+B_{22})\psi_{xj}+\sum_{j=1}^{N}(\frac{T_{22}}{x}c_{ij}^{(1)}+T_{22}c_{ij}^{(2)})\psi_{\theta j}-(\frac{m}{x\sin\alpha})\sum_{j=1}^{N}c_{ij}^{(1)}(T_{33}+B_{33})\phi_{xj}+\\
&\sum_{j=1}^{N}(\frac{T_{33}}{x}c_{ij}^{(1)}+T_{33}c_{ij}^{(2)})\phi_{\theta j}-(\frac{m}{x\sin\alpha})\sum_{j=1}^{N}c_{ij}^{(1)}(T_{44}+B_{44})\eta_{xj}+\sum_{j=1}^{N}(\frac{T_{44}}{x}c_{ij}^{(1)}+T_{44}c_{ij}^{(2)})\eta_{\theta j}=-\omega^2(I_1v_{0i}+I_2\psi_{\theta i}+I_3\phi_{\theta i}+I_4\eta_{\theta i})
\end{aligned}
\tag{A.2}
$$

$$
\begin{aligned}
&-\left(\frac{L_{11}\cos\alpha}{x^2\sin\alpha}\right)u_{0i}-(\frac{mL_{11}\cos\alpha}{x^2\sin^2\alpha}+\frac{mq_{11}\cos\alpha}{x^2\sin^2\alpha})v_{0i}-(\frac{L_{11}\cos^2\alpha}{x^2\sin^2\alpha}+\frac{m^2q_{11}}{x^2\sin^2\alpha})w_{0i}+\\
&(\frac{K_{11}}{x}-\frac{L_{22}\cos\alpha}{x^2\sin\alpha})\psi_{xi}+(-\frac{mL_{22}\cos\alpha}{x^2\sin^2\alpha}-\frac{mq_{22}\cos\alpha}{x^2\sin^2\alpha}+\frac{mq_{11}}{x\sin\alpha})\psi_{\theta i}+(\frac{2K_{22}}{x}-\frac{L_{33}\cos\alpha}{x^2\sin\alpha})\phi_{xi}\\
&+(-\frac{mL_{33}\cos\alpha}{x^2\sin^2\alpha}-\frac{mq_{33}\cos\alpha}{x^2\sin^2\alpha}+\frac{2mq_{22}}{x\sin\alpha})\phi_{\theta i}+(\frac{3K_{33}}{x}-\frac{L_{44}\cos\alpha}{x^2\sin\alpha})\eta_{xi}+\\
&(-\frac{mL_{44}\cos\alpha}{x^2\sin^2\alpha}-\frac{mq_{44}\cos\alpha}{x^2\sin^2\alpha}+\frac{3mq_{33}}{x\sin\alpha})\eta_{\theta i}-(\frac{\cos\alpha}{x\sin\alpha})\sum_{j=1}^{N}(B_{11}c_{ij}^{(1)})u_{0j}+\\
&\sum_{j=1}^{N}((\frac{K_{11}}{x})c_{ij}^{(1)}+(K_{11})c_{ij}^{(2)})w_{0j}+\sum_{j=1}^{N}((K_{11}-\frac{B_{22}\cos\alpha}{x\sin\alpha})c_{ij}^{(1)})\psi_{xj}+\sum_{j=1}^{N}((2K_{22}-\frac{B_{33}\cos\alpha}{x\sin\alpha})c_{ij}^{(1)})\phi_{xj}\\
&+\sum_{j=1}^{N}((3K_{33}-\frac{B_{44}\cos\alpha}{x\sin\alpha})c_{ij}^{(1)})\eta_{xj}=-\omega^2(I_1w_{0i})
\end{aligned}
\tag{A.3}
$$

$$
\begin{aligned}
&-\left(\frac{L_{22}}{x^2}+\frac{m^2T_{22}}{x^2\sin^2\alpha}\right)u_{0i}-(\frac{mL_{22}}{x^2\sin\alpha}+\frac{mT_{22}}{x^2\sin\alpha})v_{0i}+(-\frac{L_{22}\cos\alpha}{x^2\sin\alpha})w_{0i}-(K_{11}+\frac{L_{33}}{x^2}+\frac{m^2T_{33}}{x^2\sin^2\alpha})\psi_{xi}\\
&-(\frac{mL_{33}}{x^2\sin\alpha}+\frac{mT_{33}}{x^2\sin\alpha})\psi_{\theta i}-(2K_{22}+\frac{L_{44}}{x^2}+\frac{m^2T_{44}}{x^2\sin^2\alpha})\phi_{xi}-(\frac{mL_{44}}{x^2\sin\alpha}+\frac{mT_{44}}{x^2\sin\alpha})\phi_{\theta i}-\\
&(3K_{33}+\frac{L_{55}}{x^2}+\frac{m^2T_{55}}{x^2\sin^2\alpha})\eta_{xi}-(\frac{mL_{55}}{x^2\sin\alpha}+\frac{mT_{55}}{x^2\sin\alpha})\eta_{\theta i}+\sum_{j=1}^{N}((\frac{A_{22}}{x})c_{ij}^{(1)}+(A_{22})c_{ij}^{(2)})u_{0j}+\\
&(\frac{m}{x\sin\alpha})\sum_{j=1}^{N}c_{ij}^{(1)}(T_{22}+B_{22})v_{0j}+\sum_{j=1}^{N}c_{ij}^{(1)}(\frac{B_{22}\cos\alpha}{x\sin\alpha}-K_{11})w_{0j}+\sum_{j=1}^{N}((\frac{A_{33}}{x})c_{ij}^{(1)}+(A_{33})c_{ij}^{(2)})\psi_{xj}+\\
&(\frac{m}{x\sin\alpha})\sum_{j=1}^{N}c_{ij}^{(1)}(T_{33}+B_{33})\psi_{\theta j}+\sum_{j=1}^{N}((\frac{A_{44}}{x})c_{ij}^{(1)}+(A_{44})c_{ij}^{(2)})\phi_{xj}+(\frac{m}{x\sin\alpha})\sum_{j=1}^{N}c_{ij}^{(1)}(T_{44}+B_{44})\phi_{\theta j}+\\
&\sum_{j=1}^{N}((\frac{A_{55}}{x})c_{ij}^{(1)}+(A_{55})c_{ij}^{(2)})\eta_{xj}+(\frac{m}{x\sin\alpha})\sum_{j=1}^{N}c_{ij}^{(1)}(T_{55}+B_{55})\eta_{\theta j}=-\omega^2(I_2u_{0i}+I_3\psi_{xi}+I_4\phi_{xi}+I_5\eta_{xi})
\end{aligned}
\tag{A.4}
$$

$$
\begin{aligned}
&-\left(\frac{mL_{22}}{x^2\sin\alpha}+\frac{mT_{22}}{x^2\sin\alpha}\right)u_{0i}+(-\frac{m^2L_{22}}{x^2\sin^2\alpha}-\frac{T_{22}}{x^2}+\frac{q_{11}\cos\alpha}{x\sin\alpha}-\frac{q_{22}\cos^2\alpha}{x^2\sin^2\alpha})v_{0i}+(\frac{mq_{11}}{x\sin\alpha}-\frac{mL_{22}\cos\alpha}{x^2\sin^2\alpha}-\frac{mq_{22}\cos\alpha}{x^2\sin^2\alpha})w_{0i}\\
&-(\frac{mL_{33}}{x^2\sin\alpha}+\frac{mT_{33}}{x^2\sin\alpha})\psi_{xi}+(-q_{11}-\frac{m^2L_{33}}{x^2\sin^2\alpha}-\frac{T_{33}}{x^2}+\frac{q_{22}\cos\alpha}{x\sin\alpha}-\frac{q_{33}\cos^2\alpha}{x^2\sin^2\alpha})\psi_{\theta i}-(\frac{mL_{44}}{x^2\sin\alpha}+\frac{mT_{44}}{x^2\sin\alpha})\phi_{xi}+\\
&(-2q_{22}-\frac{m^2L_{44}}{x^2\sin^2\alpha}-\frac{T_{44}}{x^2}+\frac{3q_{33}\cos\alpha}{x\sin\alpha}-\frac{q_{44}\cos^2\alpha}{x^2\sin^2\alpha})\phi_{\theta i}-(\frac{mL_{55}}{x^2\sin\alpha}+\frac{mT_{55}}{x^2\sin\alpha})\eta_{xi}+(-3q_{33}-\frac{m^2L_{55}}{x^2\sin^2\alpha}-\frac{T_{55}}{x^2}+\\
&\frac{4q_{44}\cos\alpha}{x\sin\alpha}-\frac{q_{55}\cos^2\alpha}{x^2\sin^2\alpha})\eta_{\theta i}-(\frac{m}{x\sin\alpha})\sum_{j=1}^{N}c_{ij}^{(1)}(T_{22}+B_{22})u_{0j}+\sum_{j=1}^{N}((\frac{T_{22}}{x})c_{ij}^{(1)}+(T_{22})c_{ij}^{(2)})v_{0j}-(\frac{m}{x\sin\alpha})\sum_{j=1}^{N}c_{ij}^{(1)}(T_{33}+B_{33})\psi_{xj}\\
&+\sum_{j=1}^{N}((\frac{T_{33}}{x})c_{ij}^{(1)}+(T_{33})c_{ij}^{(2)})\psi_{\theta j}-(\frac{m}{x\sin\alpha})\sum_{j=1}^{N}c_{ij}^{(1)}(T_{44}+B_{44})\phi_{xj}+\sum_{j=1}^{N}((\frac{T_{44}}{x})c_{ij}^{(1)}+(T_{44})c_{ij}^{(2)})\phi_{\theta j}-(\frac{m}{x\sin\alpha})\sum_{j=1}^{N}c_{ij}^{(1)}(T_{55}+B_{55})\eta_{xj}+\\
&\sum_{j=1}^{N}((\frac{T_{55}}{x})c_{ij}^{(1)}+(T_{55})c_{ij}^{(2)})\eta_{\theta j}=-\omega^2(I_2v_{0i}+I_3\psi_{\theta i}+I_4\phi_{\theta i}+I_5\eta_{\theta i})
\end{aligned}
\tag{A.5}
$$

$$-\left(\frac{L_{33}}{x^2}+\frac{m^2T_{33}}{x^2\sin^2\alpha}\right)u_{0i}-(\frac{mL_{33}}{x^2\sin\alpha}+\frac{mT_{33}}{x^2\sin\alpha})v_{0i}+(-\frac{L_{33}\cos\alpha}{x^2\sin\alpha})w_{0i}-(2K_{22}+\frac{L_{44}}{x^2}+\frac{m^2T_{44}}{x^2\sin^2\alpha})\psi_{xi}$$
$$-(\frac{mL_{44}}{x^2\sin\alpha}+\frac{mT_{44}}{x^2\sin\alpha})\psi_{\theta i}-(4K_{33}+\frac{L_{55}}{x^2}+\frac{m^2T_{55}}{x^2\sin^2\alpha})\phi_{xi}-(\frac{mL_{55}}{x^2\sin\alpha}+\frac{mT_{55}}{x^2\sin\alpha})\phi_{\theta i}-(6K_{33}+\frac{L_{66}}{x^2}+\frac{m^2T_{66}}{x^2\sin^2\alpha})\eta_{xi}$$
$$-(\frac{mL_{66}}{x^2\sin\alpha}+\frac{mT_{66}}{x^2\sin\alpha})\eta_{\theta i}+\sum_{j=1}^{N}((\frac{A_{33}}{x})c_{ij}^{(1)}+(A_{33})c_{ij}^{(2)})u_{0j}+(\frac{m}{x\sin\alpha})\sum_{j=1}^{N}c_{ij}^{(1)}(T_{33}+B_{33})v_{0j}+$$
$$\sum_{j=1}^{N}c_{ij}^{(1)}(\frac{B_{33}\cos\alpha}{x\sin\alpha}-2K_{22})w_{0j}\sum_{j=1}^{N}((\frac{A_{44}}{x})c_{ij}^{(1)}+(A_{44})c_{ij}^{(2)})\psi_{xj}+(\frac{m}{x\sin\alpha})\sum_{j=1}^{N}c_{ij}^{(1)}(T_{44}+B_{44})\psi_{\theta j}+$$
$$\sum_{j=1}^{N}((\frac{A_{55}}{x})c_{ij}^{(1)}+(A_{55})c_{ij}^{(2)})\phi_{xj}+(\frac{m}{x\sin\alpha})\sum_{j=1}^{N}c_{ij}^{(1)}(T_{55}+B_{55})\phi_{\theta j}+\sum_{j=1}^{N}((\frac{A_{66}}{x})c_{ij}^{(1)}+(A_{66})c_{ij}^{(2)})\eta_{xj}+$$
$$(\frac{m}{x\sin\alpha})\sum_{j=1}^{N}c_{ij}^{(1)}(T_{66}+B_{66})\eta_{\theta j}=-\omega^2(I_3u_{0i}+I_4\psi_{xi}+I_5\phi_{xi}+I_6\eta_{xi}) \quad (A.6)$$

$$-\left(\frac{mL_{33}}{x^2\sin\alpha}+\frac{mT_{33}}{x^2\sin\alpha}\right)u_{0i}+(-\frac{m^2L_{33}}{x^2\sin^2\alpha}-\frac{T_{33}}{x^2}+\frac{2q_{22}\cos\alpha}{x\sin\alpha}-\frac{q_{33}\cos^2\alpha}{x^2\sin^2\alpha})v_{0i}+(\frac{2mq_{22}}{x\sin\alpha}-\frac{mL_{33}\cos\alpha}{x^2\sin^2\alpha}-\frac{mq_{33}\cos\alpha}{x^2\sin^2\alpha})w_{0i}$$
$$-(\frac{mL_{44}}{x^2\sin\alpha}+\frac{mT_{44}}{x^2\sin\alpha})\psi_{xi}+(-2q_{22}-\frac{m^2L_{44}}{x^2\sin^2\alpha}-\frac{T_{44}}{x^2}+\frac{3q_{33}\cos\alpha}{x\sin\alpha}-\frac{q_{44}\cos^2\alpha}{x^2\sin^2\alpha})\psi_{\theta i}-(\frac{mL_{55}}{x^2\sin\alpha}+\frac{mT_{55}}{x^2\sin\alpha})\phi_{xi}+$$
$$(-4q_{33}-\frac{m^2L_{55}}{x^2\sin^2\alpha}-\frac{T_{55}}{x^2}+\frac{4q_{44}\cos\alpha}{x\sin\alpha}-\frac{q_{55}\cos^2\alpha}{x^2\sin^2\alpha})\phi_{\theta i}-(\frac{mL_{66}}{x^2\sin\alpha}+\frac{mT_{66}}{x^2\sin\alpha})\eta_{xi}+(-6q_{44}-\frac{m^2L_{66}}{x^2\sin^2\alpha}-\frac{T_{66}}{x^2}+$$
$$\frac{5q_{55}\cos\alpha}{x\sin\alpha}-\frac{q_{66}\cos^2\alpha}{x^2\sin^2\alpha})\eta_{\theta i}-(\frac{m}{x\sin\alpha})\sum_{j=1}^{N}c_{ij}^{(1)}(T_{33}+B_{33})u_{0j}+\sum_{j=1}^{N}((\frac{T_{33}}{x})c_{ij}^{(1)}+(T_{33})c_{ij}^{(2)})v_{0j}-$$
$$(\frac{m}{x\sin\alpha})\sum_{j=1}^{N}c_{ij}^{(1)}(T_{44}+B_{44})\psi_{xj}+\sum_{j=1}^{N}((\frac{T_{44}}{x})c_{ij}^{(1)}+(T_{44})c_{ij}^{(2)})\psi_{\theta j}-(\frac{m}{x\sin\alpha})\sum_{j=1}^{N}c_{ij}^{(1)}(T_{55}+B_{55})\phi_{xj}+$$
$$\sum_{j=1}^{N}((\frac{T_{55}}{x})c_{ij}^{(1)}+(T_{55})c_{ij}^{(2)})\phi_{\theta j}-(\frac{m}{x\sin\alpha})\sum_{j=1}^{N}c_{ij}^{(1)}(T_{66}+B_{66})\eta_{xj}+\sum_{j=1}^{N}((\frac{T_{66}}{x})c_{ij}^{(1)}+(T_{66})c_{ij}^{(2)})\eta_{\theta j}=$$
$$-\omega^2(I_3v_{0i}+I_4\psi_{\theta i}+I_5\phi_{\theta i}+I_6\eta_{\theta i}) \quad (A.7)$$

$$-\left(\frac{L_{44}}{x^2}+\frac{m^2T_{44}}{x^2\sin^2\alpha}\right)u_{0i}-(\frac{mL_{44}}{x^2\sin\alpha}+\frac{mT_{44}}{x^2\sin\alpha})v_{0i}+(-\frac{L_{44}\cos\alpha}{x^2\sin\alpha})w_{0i}-(3K_{33}+\frac{L_{55}}{x^2}+\frac{m^2T_{55}}{x^2\sin^2\alpha})\psi_{xi}$$
$$-(\frac{mL_{55}}{x^2\sin\alpha}+\frac{mT_{55}}{x^2\sin\alpha})\psi_{\theta i}-(6K_{44}+\frac{L_{66}}{x^2}+\frac{m^2T_{66}}{x^2\sin^2\alpha})\phi_{xi}-(\frac{mL_{66}}{x^2\sin\alpha}+\frac{mT_{66}}{x^2\sin\alpha})\phi_{\theta i}-$$
$$(9K_{55}+\frac{L_{77}}{x^2}+\frac{m^2T_{77}}{x^2\sin^2\alpha})\eta_{xi}-(\frac{mL_{77}}{x^2\sin\alpha}+\frac{mT_{77}}{x^2\sin\alpha})\eta_{\theta i}+\sum_{j=1}^{N}((\frac{A_{44}}{x})c_{ij}^{(1)}+(A_{44})c_{ij}^{(2)})u_{0j}+$$
$$(\frac{m}{x\sin\alpha})\sum_{j=1}^{N}c_{ij}^{(1)}(T_{44}+B_{44})v_{0j}+\sum_{j=1}^{N}c_{ij}^{(1)}(\frac{B_{44}\cos\alpha}{x\sin\alpha}-3K_{33})w_{0j}\sum_{j=1}^{N}((\frac{A_{55}}{x})c_{ij}^{(1)}+(A_{55})c_{ij}^{(2)})\psi_{xj}+$$
$$(\frac{m}{x\sin\alpha})\sum_{j=1}^{N}c_{ij}^{(1)}(T_{55}+B_{55})\psi_{\theta j}+\sum_{j=1}^{N}((\frac{A_{66}}{x})c_{ij}^{(1)}+(A_{66})c_{ij}^{(2)})\phi_{xj}+(\frac{m}{x\sin\alpha})\sum_{j=1}^{N}c_{ij}^{(1)}(T_{66}+B_{66})\phi_{\theta j}$$
$$+\sum_{j=1}^{N}((\frac{A_{77}}{x})c_{ij}^{(1)}+(A_{77})c_{ij}^{(2)})\eta_{xj}+(\frac{m}{x\sin\alpha})\sum_{j=1}^{N}c_{ij}^{(1)}(T_{77}+B_{77})\eta_{\theta j}=-\omega^2(I_4u_{0i}+I_5\psi_{xi}+I_6\phi_{xi}+I_7\eta_{xi}) \quad (A.8)$$

$$-\left(\frac{mL_{44}}{x^2\sin\alpha}+\frac{mT_{44}}{x^2\sin\alpha}\right)u_{0i}+(-\frac{m^2L_{44}}{x^2\sin^2\alpha}-\frac{T_{44}}{x^2}+\frac{3q_{33}\cos\alpha}{x\sin\alpha}-\frac{q_{44}\cos^2\alpha}{x^2\sin^2\alpha})v_{0i}+(\frac{3mq_{33}}{x\sin\alpha}-\frac{mL_{44}\cos\alpha}{x^2\sin^2\alpha}-\frac{mq_{44}\cos\alpha}{x^2\sin^2\alpha})w_{0i}$$
$$-(\frac{mL_{55}}{x^2\sin\alpha}+\frac{mT_{55}}{x^2\sin\alpha})\psi_{xi}+(-3q_{33}-\frac{m^2L_{55}}{x^2\sin^2\alpha}-\frac{T_{55}}{x^2}+\frac{4q_{44}\cos\alpha}{x\sin\alpha}-\frac{q_{55}\cos^2\alpha}{x^2\sin^2\alpha})\psi_{\theta i}-(\frac{mL_{66}}{x^2\sin\alpha}+\frac{mT_{66}}{x^2\sin\alpha})\phi_{xi}+$$
$$(-6q_{44}-\frac{m^2L_{66}}{x^2\sin^2\alpha}-\frac{T_{66}}{x^2}+\frac{5q_{55}\cos\alpha}{x\sin\alpha}-\frac{q_{66}\cos^2\alpha}{x^2\sin^2\alpha})\phi_{\theta i}-(\frac{mL_{77}}{x^2\sin\alpha}+\frac{mT_{77}}{x^2\sin\alpha})\eta_{xi}+(-9q_{55}-\frac{m^2L_{77}}{x^2\sin^2\alpha}-\frac{T_{77}}{x^2}+$$
$$\frac{6q_{66}\cos\alpha}{x\sin\alpha}-\frac{q_{77}\cos^2\alpha}{x^2\sin^2\alpha})\eta_{\theta i}-(\frac{m}{x\sin\alpha})\sum_{j=1}^{N}c_{ij}^{(1)}(T_{44}+B_{44})u_{0j}+\sum_{j=1}^{N}((\frac{T_{44}}{x})c_{ij}^{(1)}+(T_{44})c_{ij}^{(2)})v_{0j}-(\frac{m}{x\sin\alpha})\sum_{j=1}^{N}c_{ij}^{(1)}(T_{55}+B_{55})\psi_{xj}$$
$$+\sum_{j=1}^{N}((\frac{T_{55}}{x})c_{ij}^{(1)}+(T_{55})c_{ij}^{(2)})\psi_{\theta j}-(\frac{m}{x\sin\alpha})\sum_{j=1}^{N}c_{ij}^{(1)}(T_{66}+B_{66})\phi_{xj}+\sum_{j=1}^{N}((\frac{T_{66}}{x})c_{ij}^{(1)}+(T_{66})c_{ij}^{(2)})\phi_{\theta j}-(\frac{m}{x\sin\alpha})\sum_{j=1}^{N}c_{ij}^{(1)}(T_{77}+B_{77})\eta_{xj}$$
$$+\sum_{j=1}^{N}((\frac{T_{77}}{x})c_{ij}^{(1)}+(T_{77})c_{ij}^{(2)})\eta_{\theta j}=-\omega^2(I_4v_{0i}+I_5\psi_{\theta i}+I_6\phi_{\theta i}+I_7\eta_{\theta i}) \quad (A.9)$$

Simply-Simply(S-S) boundary conditions at the both ends of the truncated conical shell are discretized as**:**

$$\sum_{j=1}^{N} A_{11}c_{ij}^{(1)}u_{0j} + \sum_{j=1}^{N} A_{22}c_{ij}^{(1)}\psi_{xj} + \sum_{j=1}^{N} A_{33}c_{ij}^{(1)}\phi_{xj} + \sum_{j=1}^{N} A_{44}c_{ij}^{(1)}\eta_{xj} + \frac{B_{11}}{x}u_{0i} + \frac{B_{11}m}{x\sin(\alpha)}v_{0i}$$
$$+\frac{B_{11}\cos(\alpha)}{x\sin(\alpha)}w_{0i} + \frac{B_{22}}{x}\psi_{xi} + \frac{B_{22}m}{x\sin(\alpha)}\psi_{\theta i} + \frac{B_{33}}{x}\phi_{xi} + \frac{B_{33}m}{x\sin(\alpha)}\phi_{\theta i} + \frac{B_{44}}{x}\eta_{xi} + \frac{B_{44}m}{x\sin(\alpha)}\eta_{\theta i} = 0$$
$$\sum_{j=1}^{N} A_{22}c_{ij}^{(1)}u_{0j} + \sum_{j=1}^{N} A_{33}c_{ij}^{(1)}\psi_{xj} + \sum_{j=1}^{N} A_{44}c_{ij}^{(1)}\phi_{xj} + \sum_{j=1}^{N} A_{55}c_{ij}^{(1)}\eta_{xj} + \frac{B_{22}}{x}u_{0i} + \frac{B_{22}m}{x\sin(\alpha)}v_{0i} +$$
$$\frac{B_{22}\cos(\alpha)}{x\sin(\alpha)}w_{0i} + \frac{B_{33}}{x}\psi_{xi} + \frac{B_{33}m}{x\sin(\alpha)}\psi_{\theta i} + \frac{B_{44}}{x}\phi_{xi} + \frac{B_{44}m}{x\sin(\alpha)}\phi_{\theta i} + \frac{B_{55}}{x}\eta_{xi} + \frac{B_{55}m}{x\sin(\alpha)}\eta_{\theta i} = 0$$
$$\sum_{j=1}^{N} A_{44}c_{ij}^{(1)}u_{0j} + \sum_{j=1}^{N} A_{55}c_{ij}^{(1)}\psi_{xj} + \sum_{j=1}^{N} A_{66}c_{ij}^{(1)}\phi_{xj} + \sum_{j=1}^{N} A_{77}c_{ij}^{(1)}\eta_{xj} + \frac{B_{44}}{x}u_{0i} + \frac{B_{44}m}{x\sin(\alpha)}v_{0i} +$$
$$\frac{B_{44}\cos(\alpha)}{x\sin(\alpha)}w_{0i} + \frac{B_{55}}{x}\psi_{xi} + \frac{B_{55}m}{x\sin(\alpha)}\psi_{\theta i} + \frac{B_{66}}{x}\phi_{xi} + \frac{B_{66}m}{x\sin(\alpha)}\phi_{\theta i} + \frac{B_{77}}{x}\eta_{xi} + \frac{B_{77}m}{x\sin(\alpha)}\eta_{\theta i} = 0$$
$$\sum_{j=1}^{N} A_{33}c_{ij}^{(1)}u_{0j} + \sum_{j=1}^{N} A_{44}c_{ij}^{(1)}\psi_{xj} + \sum_{j=1}^{N} A_{55}c_{ij}^{(1)}\phi_{xj} + \sum_{j=1}^{N} A_{66}c_{ij}^{(1)}\eta_{xj} + \frac{B_{33}}{x}u_{0i} + \frac{B_{33}m}{x\sin(\alpha)}v_{0i} +$$
$$\frac{B_{33}\cos(\alpha)}{x\sin(\alpha)}w_{0i} + \frac{B_{44}}{x}\psi_{xi} + \frac{B_{44}m}{x\sin(\alpha)}\psi_{\theta i} + \frac{B_{55}}{x}\phi_{xi} + \frac{B_{55}m}{x\sin(\alpha)}\phi_{\theta i} + \frac{B_{66}}{x}\eta_{xi} + \frac{B_{66}m}{x\sin(\alpha)}\eta_{\theta i} = 0 \qquad \text{(A.10)}$$

$$\sum_{j=1}^{N} T_{22}C_{ij}^{(1)}v_{0j} + \sum_{j=1}^{N} T_{33}C_{ij}^{(1)}\psi_{\theta j} + \sum_{j=1}^{N} T_{44}C_{ij}^{(1)}\phi_{\theta j} + \sum_{j=1}^{N} T_{55}C_{ij}^{(1)}\eta_{\theta j} - \frac{T_{22}m}{x\sin(\alpha)}u_{0i} - \frac{T_{22}}{x}v_{0i} -$$
$$\frac{T_{33}m}{x\sin(\alpha)}\psi_{xi} - \frac{T_{33}}{x}\psi_{\theta i} - \frac{T_{44}m}{x\sin(\alpha)}\phi_{xi} - \frac{T_{44}}{x}\phi_{\theta i} - \frac{T_{55}m}{x\sin(\alpha)}\eta_{xi} - \frac{T_{55}}{x}\eta_{\theta i} = 0$$
$$\sum_{j=1}^{N} T_{33}C_{ij}^{(1)}v_{0j} + \sum_{j=1}^{N} T_{44}C_{ij}^{(1)}\psi_{\theta j} + \sum_{j=1}^{N} T_{55}C_{ij}^{(1)}\phi_{\theta j} + \sum_{j=1}^{N} T_{66}C_{ij}^{(1)}\eta_{\theta j} - \frac{T_{33}m}{x\sin(\alpha)}u_{0i} - \frac{T_{33}}{x}v_{0i} -$$
$$\frac{T_{44}m}{x\sin(\alpha)}\psi_{xi} - \frac{T_{44}}{x}\psi_{\theta i} - \frac{T_{55}m}{x\sin(\alpha)}\phi_{xi} - \frac{T_{55}}{x}\phi_{\theta i} - \frac{T_{66}m}{x\sin(\alpha)}\eta_{xi} - \frac{T_{66}}{x}\eta_{\theta i} = 0$$
$$\sum_{j=1}^{N} T_{44}C_{ij}^{(1)}v_{0j} + \sum_{j=1}^{N} T_{55}C_{ij}^{(1)}\psi_{\theta j} + \sum_{j=1}^{N} T_{66}C_{ij}^{(1)}\phi_{\theta j} + \sum_{j=1}^{N} T_{77}C_{ij}^{(1)}\eta_{\theta j} - \frac{T_{44}m}{x\sin(\alpha)}u_{0i} - \frac{T_{44}}{x}v_{0i} -$$
$$\frac{T_{55}m}{x\sin(\alpha)}\psi_{xi} - \frac{T_{55}}{x}\psi_{\theta i} - \frac{T_{66}m}{x\sin(\alpha)}\phi_{xi} - \frac{T_{66}}{x}\phi_{\theta i} - \frac{T_{77}m}{x\sin(\alpha)}\eta_{xi} - \frac{T_{77}}{x}\eta_{\theta i} = 0$$
$$v_{0i} = 0$$
$$w_{0i} = 0 \qquad i = 1, N$$

REFERENCES

[1] Malekzadeh P., 2009, Three-dimensional free vibration analysis of thick functionally graded plates on elastic foundations, *Composite Structures* **89**: 367-373.

[2] Hosseini-Hashemi Sh., Rokni H., Damavandi T., Akhavan H., Omidi M., 2010, Free vibration of functionally graded rectangular plates using first-order shear deformation plate theory, *Applied Mathematical Modelling* **34**: 1276-1291.

[3] Pan E., Han F., 2005, Exact solution for functionally graded and layered magnetoelectro- elastic plates, *International Journal of Engineering Science* **43**: 321-339.

[4] Yas M.H., Sobhani Aragh B., 2010, Free vibration analysis of continuously graded fiber reinforced plates on elastic foundation, *International Journal of Engineering Science* **48**: 1881-1895.

[5] Chen W.Q., 2000, Vibration theory of non-homogeneous, spherically isotropic piezoelastic bodies, *Journal of Sound and Vibration* **229**: 833-860.

[6] Chiroiu V., Munteanu L., 2007, On the free vibrations of a piezoceramic hollow sphere, *Mechanics Research Communications* **34**: 123-129.

[7] Bahtui A., Eslami M.R., 2007, Coupled thermoelasticity of functionally graded cylindrical shells, *Mechanics Research Communications* **34**: 1-18.

[8] Haddadpour H., Mahmoudkhani S., Navazi H.M., 2007, Free vibration analysis of functionally graded cylindrical shells including thermal effects, *Thin-Walled Structures* **45**: 591-599.

[9] Sobhani Aragh B., Yas M.H., 2010, Static and free vibration analyses of continuously graded fiber-reinforced cylindrical shells using generalized power-law distribution, *Acta Mechanica* **215**: 155-173.

[10] Sobhani Aragh B., Yas M.H., 2010, Three-dimensional analysis of thermal stresses in four-parameter continuous grading fiber reinforced cylindrical panels, *International Journal of Mechanical Sciences* **52**: 1047-1063.

[11] Sobhani Aragh B., Yas M.H., 2010, Three-dimensional free vibration of functionally graded fiber orientation and volume fraction cylindrical panels, *Materials & Design* **31**: 4543-4552.
[12] Yas M.H., Sobhani Aragh B., 2010, Three-dimensional analysis for thermoelastic response of functionally graded fiber reinforced cylindrical panel, *Composite Structures* **92**: 2391-2399.
[13] Thambiratnam D., Zhuge Y., 1993, Axisymmetric free vibration analysis of conical shells, *Engineering Structures* **15**(2): 83-89.
[14] Tong L., 1993, Free vibration of orthotropic conical shells, *International Journal of Engineering Science* **31**(5): 719-733.
[15] Leissa A., 1993, *Vibration of Shells*, The Acoustic Society of America.
[16] Liew K.M., Lim C.W., 1994, Vibratory characteristics of cantilevered rectangular shallow shells of variable thickness, *The American Institute of Aeronautics and Astronautics* **32**(3): 87-96.
[17] Liew K.M., Lim C.W.. 1994, Vibration of perforated doubly-curved shallow shells with rounded corners, *International Journal of Solids and Structures* **31**(15): 19-36.
[18] Shu C., 1996, Free vibration analysis of composite laminated conical shells by generalized differential quadrature, *Journal of Sound and Vibration* **194**: 587-604.
[19] Bardell N.S., Dunsdon J.M., Langley R.S., 1998, Free vibration of thin, isotropic, open, conical panels, *Journal of Sound and Vibration* **217**: 297-320.
[20] Wang Y., Liu R., Wang X., 1999, Free vibration analysis of truncated conical shells by the Differential Quadrature Method, *Journal of Sound and Vibration* **224**(2): 387-394.
[21] Sofiyev A.H., 2009, The vibration and stability behavior of freely supported FGM conical shells subjected to external pressure, *Composite Structures* **89**(3): 56-66.
[22] Liew K.M., Ng T.Y., Zhao X., 2005, Free vibration analysis of conical shells via the element-free kp-Ritz method, *Journal of Sound and Vibration* **281**: 627-645.
[23] Bhangale R.K., Ganesan N., Padmanabhan C., 2006, Linear thermoelastic buckling and free vibration behavior of functionally graded truncated conical shells, *Journal of Sound and Vibration* **292**: 341-371.
[24] Tornabene F., 2009, Free vibration analysis of functionally graded conical, cylindrical shell and annular plate structures with a four-parameter power-law distribution, *Computer Methods in Applied Mechanics and Engineering* **198**: 2911-2935.
[25] Malekzadeh P., Fiouz A.R., Sobhrouyan M., 2012, Three-dimensional free vibration of functionally graded truncated conical shells subjected to thermal environment, *International Journal of Pressure Vessels and Piping* **89**: 210-221.
[26] Sofiyev A.H., 2012, The non-linear vibration of FGM truncated conical shells, *Composite Structures* **94**: 2237-2245.
[27] Reddy J.N., 1984, A refined nonlinear theory of plates with transverse shear deformation, *International Journal of Solids and Structures* **20**: 881-896.
[28] Lee Y.S., Lee K.D., 1997,On the dynamic response of laminated circular cylindrical shells under impulse loads, *Computers & Structures* **63**(1): 149-157.
[29] Khalili S.M.R., Malekzadeh K., Davar A., Mahajan P., 2010, Dynamic response of pre-stressed fibre metal laminate (FML) circular cylindrical shells subjected to lateral pressure pulse loads, *Composite Structures* **92**: 1308-1317.
[30] Vasiliev V.V., Morozov E.V., 2001, *Mechanics and Analysis of Composite Materials*, Elsevier Science.
[31] Bert C.W., Malik M., 1996, Differential quadrature method in computational mechanics, a review, *Journal of Applied Mechanic* **49**: 1-27.
[32] Irie T., Yamada G., Tanaka K., 1984, Natural frequencies of truncated conical shells, *Journal of Sound and Vibration* **92**: 447-453.